

## On X-ray Variability in Active Binary Stars

Vinay Kashyap<sup>1</sup> and Jeremy J. Drake<sup>2</sup>

<sup>1</sup>Harvard-Smithsonian Center for Astrophysics, MS-83,  
60 Garden Street,  
Cambridge, MA 02138

<sup>2</sup>Harvard-Smithsonian Center for Astrophysics, MS-3,  
60 Garden Street,  
Cambridge, MA 02138

### ABSTRACT

We have compared the X-ray emissions of active binary stars observed at various epochs by the *Einstein* and *ROSAT* satellites in order to investigate the nature of their X-ray variability. The main aim of this work is to determine whether or not active binaries exhibit long-term variations in X-ray emission, perhaps analogous to the observed cyclic behavior of solar magnetic activity. We find that, while the mean level of emission of the sample remains steady, comparison of different *ROSAT* observations of the same stars shows significant variation on timescales  $\lesssim 2$  yr, with an “effective variability”  $\frac{\Delta I}{I} = 0.32 \pm 0.04$ , where  $I$  and  $\Delta I$  represent the mean, and variation from the mean, emission, respectively. A comparison of *ROSAT* All-Sky Survey and later pointed observations with earlier observations of the same stars carried out with *Einstein* yields only marginal evidence for a larger variation ( $\frac{\Delta I}{I} = 0.38 \pm 0.04$  for *Einstein* vs. *ROSAT* All-Sky Survey and  $0.46 \pm 0.05$  for *Einstein* vs. *ROSAT* pointed) at these longer timescales ( $\sim 10$  yr), indicating the possible presence of a long-term component to the variability.

Whether this long-term component is due to the presence of cyclic variability cannot be decided on the basis of existing data. However, assuming that this component is analogous to the observed cyclic variability of the Sun, we find that the relative magnitude of the cyclic component in the *ROSAT* passband can at most be a factor of 4, i.e.,  $\frac{I_{cyc}}{I_{min}} < 4$ . This is to be compared to the corresponding – significantly higher – solar value of  $\sim 10 - 10^2$  derived from GOES, Yohkoh, and Solrad data. These results are consistent with the suggestions of earlier studies that a turbulent or distributive dynamo might be responsible for the observed magnetic activity on the most active, rapidly rotating stars.

*Subject headings:* X-rays: stars: activity, stars: binaries, stars: coronae, stars: statistics, stars: variables: other, X-rays: stars

## 1. Introduction

Observations of the solar corona over timescales of years have shown the coronal X-ray emission, together with other indicators of activity such as Ca II H and K emission line strength, to be modulated by the solar dynamo on the 22 year magnetic field polarity reversal cycle, with maxima and minima occurring every 11 years or so (e.g., see the review by Harvey 1992). Surveys of the X-ray sky performed by the *Einstein Observatory*, and later by *EXOSAT* and *ROSAT*, have also firmly established the existence of supposedly analogous hot X-ray emitting coronae throughout the late main sequence (F-M), and also in late-type giants down to spectral types near mid-K (e.g., Vaiana et al. 1981). One fundamental issue in stellar physics concerns the relationship between this magnetic activity on stars with a wide range of physical parameters and solar magnetic activity (see review by Saar & Baliunas 1992): how directly and how far does the solar analogy apply to other stars, and how do the underlying physical processes differ? Unfortunately, while stellar coronal X-ray emission has been known and studied for more than 20 years, the small number of satellites in orbit at any given time able to observe it severely limits our knowledge of any long-term trends in stellar X-ray activity. Such knowledge is currently restricted to a handful of stars caught during repeated brief snapshots of them afforded by observations of different satellites.

If magnetic cycles with similar timescales to that of the Sun are present on other stars, as convincing evidence from the long-term Mt. Wilson Ca II H+K monitoring program suggests (e.g., Baliunas et al. 1995 and references therein), then one might also expect these stars to modulate their coronal X-ray fluxes in a similar way to the Sun. Further, on the Sun these modulations are large: Solrad observations (Kreplin 1970) in the 44-60Å and 8-20Å passbands show that X-ray flux at activity maximum (c.1968) is  $\sim 20$  and  $\gtrsim 200$  times greater than at activity minimum (July 1964) respectively (see also Vaiana & Rosner 1978). Also, as stated by Hempelmann, Schmitt & Stèpièn (1996), the variation of the solar X-ray flux in the equivalent of the *ROSAT*/PSPC bandpass over its activity cycle is a factor of 10 or more (also Pallavicini 1993; but Ayres et al. 1996, extrapolating from XUV data predict a variation by only a factor  $\sim 4$ ), similar to the ratio deduced for the variations in the soft X-ray range of *Yohkoh* based on ratios of X-ray fluxes in the 1-8Å passband of GOES (Aschwanden 1994), and as also directly observed by *Yohkoh* (Acton 1996). Such large long-term changes in mean stellar X-ray flux levels are, at least in principle, easily detectable. However, studies of stellar X-ray emission at different epochs based on *Einstein* and subsequent *ROSAT* observations of stars in open clusters (Stern et al. 1995, Gagné et al. 1995; Micela et al. 1996), as well as field stars (Schmitt, Fleming, & Giampapa 1995, Fleming et al. 1995) suggest that these active stars, at least, do not show strong long-term components of variability; some of these results are discussed by Stern (1998). A recent study by Hempelmann et al. (1996) of F-K main sequence stars also finds that the more active stars with higher surface X-ray fluxes tend not to have well-defined cyclic activity in terms of the Ca II H+K activity index. Some authors have suggested that this lack of clear detection of activity cycles might be an observational consequence of the dominant magnetic activity on the more active stars being due

to a different dynamo process to the solar large-scale field  $\alpha\omega$  dynamo (e.g., Stern et al. 1995; Drake et al. 1996).

In this paper, we turn to the most active stars – the RSCVn and BY Dra binaries – in order to investigate whether or not they might exhibit some form of cyclic, or other long-term variability in their X-ray emission. We look at a sample of active binary stars that have been detected by the *Einstein Observatory* (c.1978-81) and that have also been observed by the *ROSAT*/PSPC both during the all-sky survey (c.1990), and during later pointed observations (c.1991-1994). We compare the different observations in order to assess whether or not there is any significant difference between *changes* in flux levels over short-term timescales ( $\sim \frac{1}{2} - 2$  yrs; *ROSAT* All-Sky Survey v/s pointed phase) compared with changes over longer-term timescales ( $\sim 10 - 12$  yrs; *ROSAT* v/s *Einstein*).

In §2 we describe the star sample used in this study. In §3 we describe the statistical method we adopt to compare the samples and discuss the implications of our results: in §3.1 we consider the correlations of the samples and their deviations from equality; in §3.2 we discuss the statistical significance of the analysis; and in §3.3 we discuss the implications of our results in the context of stellar activity cycles. We summarize in §4.

## 2. Data Selection

We adopt the sample of 206 spectroscopic binary systems of Strassmeier et al. (1993) as our baseline database of active stars. This sample was selected by Strassmeier et al. such that each system has at least one late-type component that shows Ca II H and K emission in its spectrum.

In Table 1 we list a subset of the Strassmeier et al. stars which have at least one X-ray measurement with either the *Einstein*/IPC or the *ROSAT*/PSPC, together with the relevant observed count rates. We have used the widely available catalogs of the *Einstein* Slew Survey (“Slew”; Elvis et al. 1992, Plummer et al. 1994), the *Einstein* Extended Medium Sensitivity Survey (“EMSS”; Gioia et al. 1990, Stocke et al. 1991), and the *Einstein*/IPC Source Catalog (“EOSCAT”; Harris et al. 1990) to obtain *Einstein*/IPC measurements (“Einstein”); and the *ROSAT* All-Sky Survey (RASS) Bright Source Catalog (“RASSBSC”; Voges et al. 1996) and *ROSAT* public archive pointed data sets (“WGACAT”; White, Giommi, & Angelini 1994) to obtain the PSPC measurements. We have not augmented the WGACAT with independently measured fluxes in order to keep the X-ray sample homogeneous.<sup>1</sup>

If a particular star is found in more than one *Einstein* survey catalog, we adopt the count rate derived in EOSCAT over that of EMSS over that of Slew. If multiple PSPC pointings exist of a star, then we use only the measurement with the highest effective exposure (including vignetting)

---

<sup>1</sup>Using other existing catalogs (e.g., “ROSATSRC”; Voges et al. 1994) of *ROSAT* pointed data sets does not change the overlaps (cf. Table 2) significantly.

and the one closest to the field-center.

In comparing *Einstein*/IPC counts with *ROSAT*/PSPC counts of the same star, we adopt a conversion factor  $\frac{PSPC}{IPC} = 3.7$  based on a straight line fit to the Einstein-RASSBSC sample. Clearly, this is an approximate number that could vary according to the adopted plasma temperature, the metallicity of the corona, and column density of absorption to the source. The bandpasses and effective areas of both instruments are however similar enough over the temperature range of interest that the ratio of count rates are insensitive to these parameters (see §3.2). RASSBSC and WGACAT counts are extracted in slightly different passbands, and an appropriate correction ( $\sim 20\%$ ) has also been applied to these datasets.

### 3. Analysis and Discussion

Subsets of the active binary stars that have been observed in two different epochs allow us to deduce the magnitude of the variability at different timescales. We begin by assuming that each such sample is statistically random, i.e., that there are no systematic changes in the variability of the sample from one epoch to the other, or in other words, that on average any increases in intrinsic luminosity is balanced by decreases in intrinsic luminosity. This assumption is supported by the Kruskal-Wallis test for both the combined samples (i.e., active binaries with X-ray data at all 3 epochs) and for the individual samples (active binaries observed in any of the 3 epochs): the hypothesis that the samples have the same mean cannot be rejected (the probability of obtaining the observed value of the K-W test statistic by chance is  $0.84 \pm 0.02$  and  $0.4 \pm 0.06$  respectively, much higher than an acceptable threshold of 0.05).<sup>2</sup> This result also confirms that the conversion factors correcting the passband differences between the catalogs have been properly evaluated.

We ignore censored data (stars detected in one survey but not in another [11 in Einstein, 3 in WGACAT, 65 in RASSBSC], as well as stars not detected in any survey [29]) in this work. The large dynamic range of the observed count rates ( $> 10^2$ ; cf. Figures 1-3) in the samples, and the strong correlations in the *detected* count rates show that ignoring undetected stars will not affect the results presented here. Further note that we use a sample that is *not* X-ray selected, and thus avoid the problem encountered by Fleming et al. (1995) who found general decreases in overall flux between *Einstein* and *ROSAT* measurements due to preferential detection of stars while flaring.

In the following sections we analyze the paired samples in greater detail (§3.1), assess the significance of our results (§3.2), and discuss the results in the context of stellar activity cycles (§3.3).

---

<sup>2</sup>Fleming et al. (1995) noted an increase in the mean X-ray emission level of a small, X-ray selected, sample of RSCVn and WUMa binaries between the *Einstein* and *ROSAT* epochs. However, the sample of stars used here has very little overlap with the Fleming et al. sample and is furthermore much larger in size and significant changes in the observed mean X-ray emission level are not expected.

### 3.1. Correlations and Deviations

The sample of stars able to shed light on “short” timescale ( $\sim 0 - 3$  yr) variability, i.e., stars re-observed after a short interval, are those active binaries present in both the RASSBSC and WGACAT, while there are two sets of paired datasets defining the “long” timescales ( $\gtrsim 10$  yr) – Einstein-RASSBSC and Einstein-WGACAT. These paired samples are shown in Figures 1-3: it is clear that the count rates are strongly correlated as one would expect in the case where intrinsic variability of a single star is much smaller than the range in brightness of the whole sample. For completeness, and to define the strength of the correlations in count rates, we have performed standard statistical correlation tests, the results of which are listed in Table 2. We have tested the sensitivity of the derived correlation coefficients to the statistical errors on the observed count rates by performing monte carlo simulations. These involved generating a new set of count rates (of the same sample size) for each star by sampling from a Gaussian with a mean identical to the observed value and standard deviation equal to the observed  $1\sigma$  error; correlation coefficients are then derived using the new set of simulated count rates. We find that the derived coefficients are stable to within  $\lesssim 0.01$ .

The strong correlations within the paired samples imply that any actual variability in X-ray emission within the sample is not much larger than the measurement errors. Indeed, the majority of the observed count rates in the different samples are within a factor of 2 of each other (after allowing for the conversion between the *Einstein* and *ROSAT* passbands). This result is similar to other comparisons of *Einstein* and *ROSAT* observations of samples of mostly active late-type stars (e.g., Schmitt et al. 1995; Stern et al. 1995; Gagné et al. 1995; Micela et al. 1996; Fleming et al. 1995). However, the larger scatter apparent in the Einstein-RASSBSC (and to a lesser extent, Einstein-WGACAT) samples compared to the RASSBSC-WGACAT sample (cf. Figures 1-3) does appear to indicate the presence of some non-statistical scatter in the data. In the following, we quantify this apparent variability.

The issue we seek to address is the extent of the departure of a paired set of count rates from strict equality. Further, any measure of this departure must include the effects of the statistical uncertainties associated with the observed count rates. Thus, we define the quantity

$$\delta_{\perp} = \frac{1}{N_{samp}} \sum_{smp} \frac{D_{\perp}}{\sigma_{tot}} \quad (1)$$

where  $D_{\perp}$  is the *perpendicular* distance of the pair of count rates from a straight line of unit slope passing through the origin, and  $\sigma_{tot}$  is the total error associated with that pair as obtained by propagating the individual errors, and  $N_{samp}$  is the number of paired count rates in the sample; if the count rates in the two samples are identical  $\delta_{\perp} = 0$ , and in the case of only statistical variations,  $\delta_{\perp} \sim 1$ . Note that this is similar (but differs in the use of perpendicular deviations and division by the error) to the merit-function used to derive straight-line fits to data such that *absolute deviation* is minimized (cf. Press et al. 1992). In the case of small deviations,  $D_{\perp}$  may be

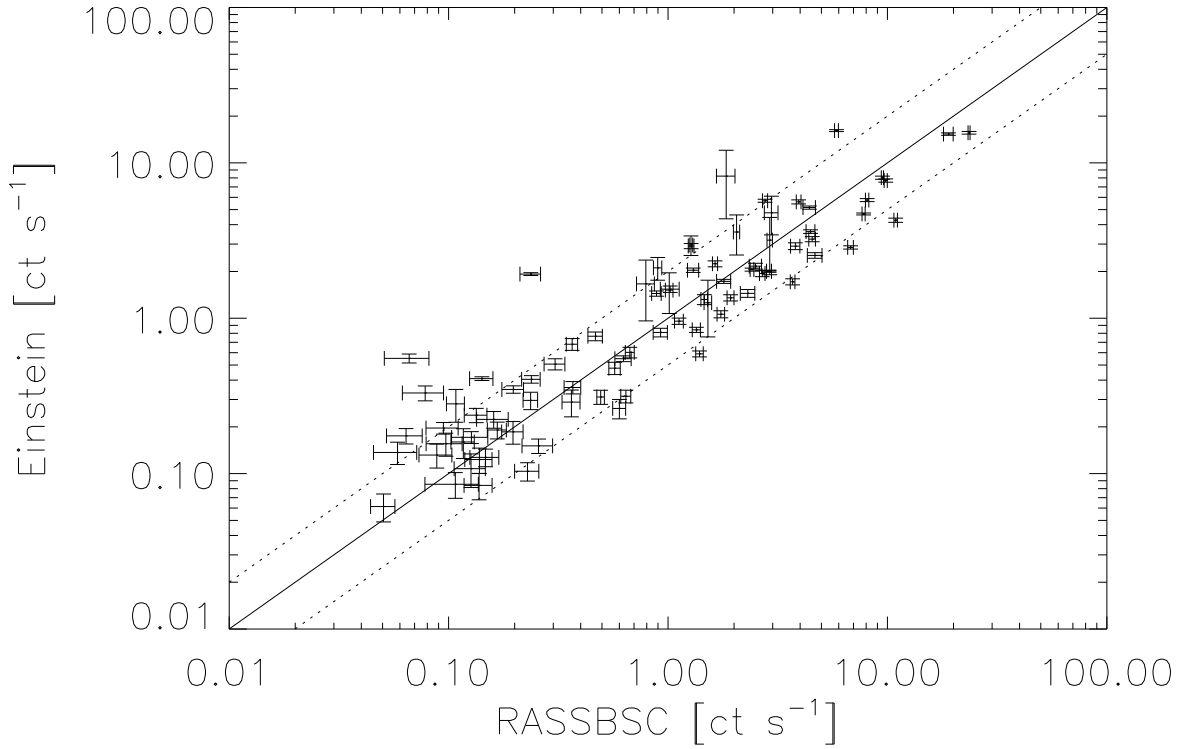


Fig. 1.— Scatter plot of count rates observed at different epochs: RASSBSC v/s Einstein. The Einstein count rates have been uniformly multiplied by a factor of 3.7 as derived by a straight-line fit to the Einstein-RASSBSC dataset. The size of the  $1\sigma$  errors on the rates is indicated by the horizontal and vertical lines at each point. The solid inclined line represents the line of equality and the dotted lines flanking it represent variations of factors of 2.

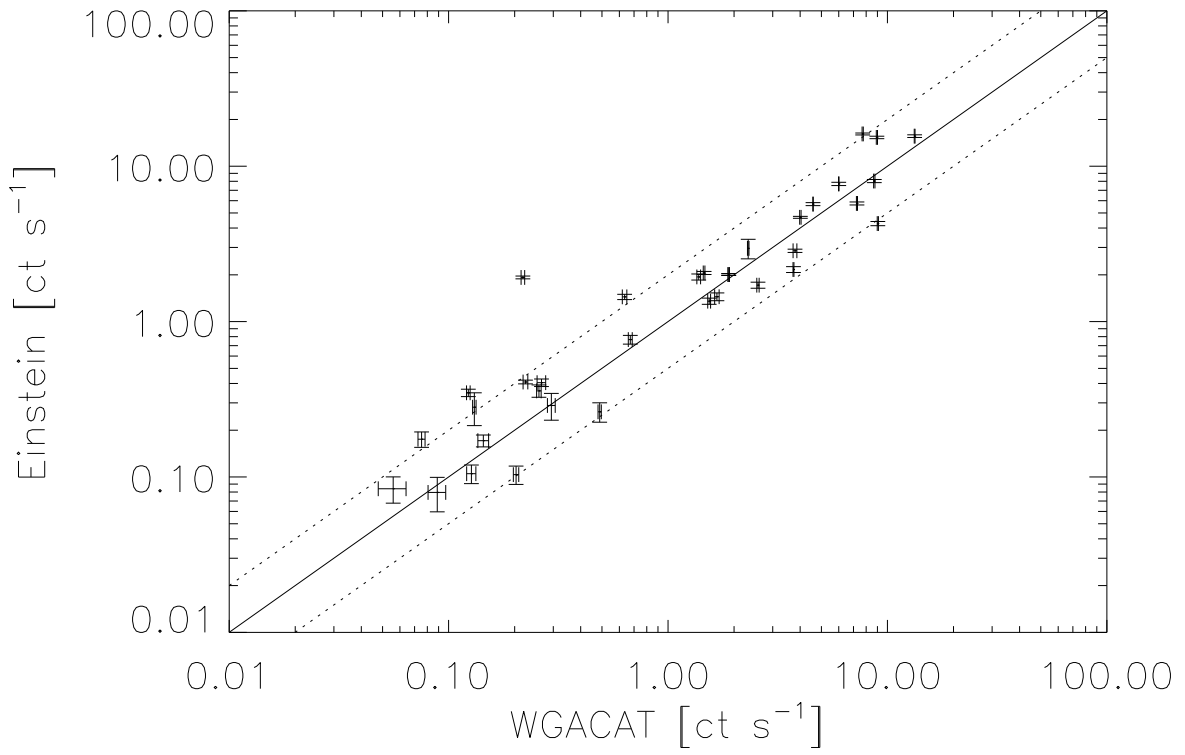


Fig. 2.— As in Figure 1, for the Einstein-WGACAT sample.

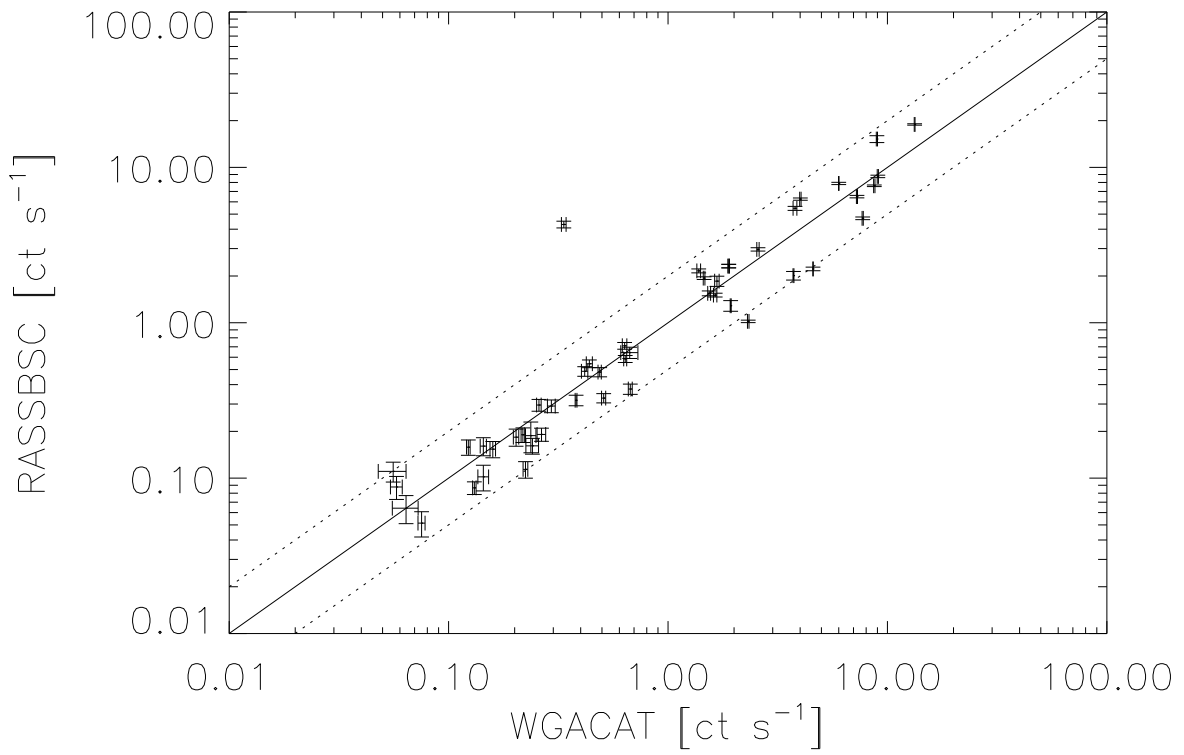


Fig. 3.— As in Figure 1, for the RASSBSC-WGACAT sample. The scatter is much less pronounced except for the sole outlier, FF Aqr.



obtained from the logarithmic ratio of the count rates.<sup>3</sup> Note that standard statistical measures such as the Students T, the F-statistic, the Sign test, etc. apply to the means and variances of the samples, and are not sensitive enough for our purposes. The adopted method also has the advantage of allowing us to parameterize the detected variability (albeit crudely; see §3.2). The values of  $\delta_{\perp}$  derived from the three pairs of datasets as defined in Equation 1 are listed in Table 3. The uncertainties in the derived values of  $\delta_{\perp}$  have been estimated from monte carlo simulations of the different datasets as described above:  $\delta_{\perp}$  was calculated for each realization of the datasets, and the estimated uncertainties correspond to the standard deviation of the simulated values of  $\delta_{\perp}$ .

In Figure 4, we show the cumulative distribution of  $D_{\perp}/\sigma_{tot}$  computed for each paired dataset, augmented by monte carlo simulations performed as described above in order to illustrate the distributions more clearly. The fraction of stars in each sample with normalized perpendicular deviates  $> D_{\perp}/\sigma_{tot}$  are shown. When the differences between two samples may be attributed solely to statistical errors, the differential distribution of normalized perpendicular deviates are distributed as a one-sided Gaussian; this distribution is also illustrated in Figure 4. Any “excess variability” – deviates larger than expected on purely statistical grounds or systematic errors – manifest themselves in the form of wider distributions, i.e., with a larger fraction of stars in the sample showing perpendicular deviates at larger values of  $D_{\perp}/\sigma_{tot}$ . Based on Figure 4, each of the samples considered shows clear and unambiguous signatures of excess variability. Indeed, 30% of the stars in the Einstein-RASSBSC sample, 45% of those in the Einstein-WGACAT sample, and 35% of those in the RASSBSC-WGACAT sample show scatter attributable to non-statistical variability at a level  $> 5\sigma$ .

We have also carried out a similar analysis on subsamples of the largest of our three samples (Einstein-RASSBSC) in order to investigate whether or not there are any trends in  $D_{\perp}/\sigma_{tot}$  with spectral type or luminosity class. We find that the resulting distributions of  $D_{\perp}/\sigma_{tot}$  are similar to the distribution obtained for the full sample, indicating that in our data there is no significant evidence for such systematic changes in observed scatter or variability in soft X-ray emission.

One of the primary goals of this study is to look for evidence of underlying variability with characteristic timescales of order a decade or so, similar to that of the solar cycle. In the case of the Sun, such variability in soft X-rays is about an order of magnitude (e.g., Pallavicini 1993, Hempelmann et al. 1996) or more (Kreplin 1970, Aschwanden 1994, Acton 1996). If such a component of variability were present in the stars of our active binary sample, we would expect the

---

<sup>3</sup>This is the statistic adopted by Gagné et al. (1995). Taking the count rates observed at two epochs to be  $c_1$  and  $c_2$ , with  $c_1 = c_2 + \delta_{12}$ ,  $\ln\left(\frac{c_1}{c_2}\right) \sim \ln\left(1 + \frac{\delta_{12}}{c_2}\right) \sim \frac{\delta_{12}}{c_2} \sim \frac{D_{\perp}}{c_2}$ . Note that this formulation preserves sign information (i.e., whether the first or the second epoch has the higher count rate; the expectation value of this statistic is 0 in the absence of variability, unlike that of  $\delta_{\perp}$  which has an expectation value  $\sim 1$ ). However, since we are only interested in deviations from constancy, we essentially marginalize over this two-sidedness (and thereby improve our detection efficiency) by using the perpendicular deviates  $D_{\perp}$ . Using the perpendicular deviates also allows us to include the effects of the measurement uncertainties in a straightforward fashion.

two *Einstein-ROSAT* samples to exhibit a larger spread in  $D_{\perp}/\sigma_{tot}$  than the RASSBSC-WGACAT sample, since the *Einstein* and *ROSAT* respective observations span an interval more comparable to the expected period of the long-term variability. That such a signature is not easily discernible may be partly attributed to the generally larger errors associated with the *Einstein* measurements of count rates—note that the perpendicular deviates considered here are normalized relative to the estimated statistical error. Thus, in order to show a similar effect as the RASSBSC-WGACAT sample, the *Einstein-ROSAT* samples must have a correspondingly larger intrinsic non-statistical differences. However, as we have emphasized above, soft X-ray variability over the solar cycle amounts to an order of magnitude or more, which is well beyond the statistical uncertainties in the *Einstein-ROSAT* comparisons. Therefore, if any long-term, or cyclic, component of variability is present in the stars of our active binary sample, then the amplitude of this variability must be much less than in the solar case. In the following sections we discuss the implications of this result.

### 3.2. Stochastic Variability

The derived values of  $\delta_{\perp}$  (see Table 3) conclusively show that the data are inconsistent, at a very high significance, with the hypothesis that there are only statistical variations in count rates among the 3 datasets acquired at different epochs: i.e., we unambiguously detect the existence of excess variation among the samples.

The nature of this excess scatter is however not as well-determined. We rule out instrumental effects as being the main cause of the observed scatter since it is seen even in the RASSBSC-WGACAT sample. In the cases involving the IPC, we note that even though the passbands and instrument sensitivities of *Einstein* and *ROSAT* differ, for spectra generated from thermal plasma at temperatures between  $5 \times 10^6$  and  $\lesssim 10^7$  K, which are the likely coronal temperatures of the stars being considered (e.g., Schmitt et al. 1990, Dempsey et al. 1993), these differences are small (cf. Wood et al. 1995) and the maximum error we are likely to make in the  $\frac{PSPC}{IPC}$  count-ratio is  $\sim 10\%$ . monte carlo simulations of the datasets including this type of error show that its effect on the value of  $\delta_{\perp}$  is to offset it by  $\sim 0.2$  and is hence negligible. We therefore conclude that the origin of the detected excess variations is intrinsic.

We now investigate the possibility that all of the observed excess variation can be attributed to stochastic variability, and then whether or not we can discern any differences in the magnitude of such variabilities between the different pairs of data (i.e., stars common to [Einstein,RASSBSC], [Einstein,WGACAT], or [RASSBSC,WGACAT]). This is not entirely straightforward because the three sets of observations were obtained under different conditions and with different instrumentation and have different measurement uncertainties. To do this we first assume that the variability detected here may be parameterized by modeling it as purely stochastic variability, relative to the estimated statistical error. We emphasize that we carry out this modeling only as a means to explore the range of  $\delta_{\perp}$ , and that it is not our intention to claim that intrinsic variability in active binaries indeed follows this pattern. We assume that the variability may be characterized

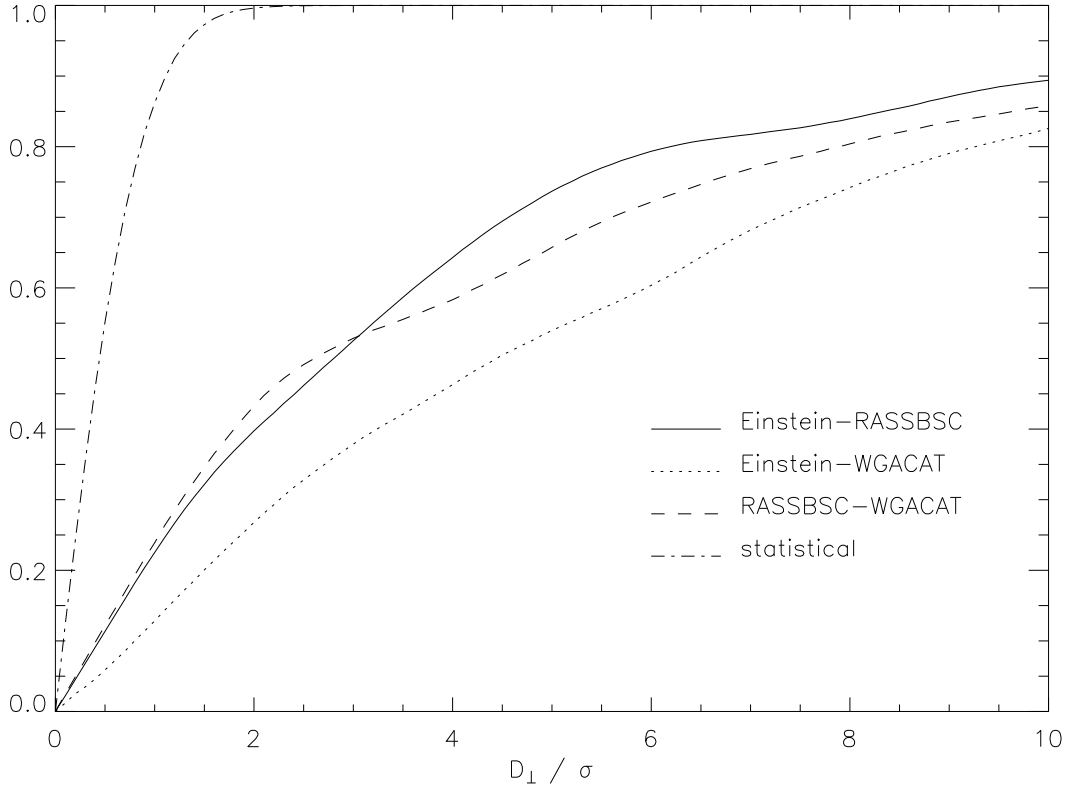


Fig. 4.— Distribution of perpendicular deviates: the fraction of stars in a given sample with deviates  $\geq \frac{D_{\perp}}{\sigma}$  is shown. In the presence of only statistical variations, the differential distribution of  $\frac{D_{\perp}}{\sigma}$  is a one-sided Gaussian, indicated here by the dash-dotted line. The presence of variability in excess of statistical deviations in a chosen sample will result in a larger fraction of the sample showing perpendicular deviates at much larger values of  $\sigma$ , as is the case for the Einstein-RASSBSC (solid stepped line), Einstein-WGACAT (dotted stepped line), and RASSBSC-WGACAT (dashed stepped line) samples; note that  $\sim 30$ ,  $45$ , and  $35\%$  of the stars in the respective samples show variability in excess of  $5\sigma$ .

by the parameter  $\beta = \frac{\Delta I}{\sigma_I}$ , where here  $\Delta I$  represents the effective change in soft X-ray emission from one observation to the next;  $\beta$  then represents the ratio of the magnitude of the variation and the observed error in the count rate. Note that this assumption obviously underestimates the magnitude of *cyclic* variability, but is adequate to summarize our results given the absence of detailed time traces of photometric and X-ray brightness of the stars in the sample. For the parameter  $\beta$  to be physically meaningful, the estimated errors must be insensitive to distance effects – i.e., the expected variability must not be a function of our special location. For the stellar sample in question (Table 1), we note that the X-ray luminosity spans a range  $\frac{max}{min}[L_x] \approx 17400$ , much greater than distance induced flux variations ( $\frac{max}{min}[d^2] \approx 4700$ ). The spread in count rates is therefore much larger than variations induced by stellar distance (and errors therein); the bias introduced into the analysis due to farther sources being weaker and thus naturally having larger relative errors is thus minimized, and the adopted parameter is a reasonable quantity to use to describe the samples. Comparison of  $\beta$  derived from different datasets is however still subject to the problem of different datasets having different relative errors, and we account for this later.

We derive the appropriate value of  $\beta$  for each dataset pair as follows. Starting from an arbitrary sample of count rates (we used RASSBSC because it is the largest sample) and an assumed value of  $\beta$ , we generated using monte carlo simulations two new sets of count rates for each point. The new count rates were obtained by sampling from two Gaussians, both with means equal to the original count rate but with different standard deviations  $\sigma_1 = \sigma_{tot}$ , the estimated statistical error (see Equation 1), and  $\sigma_2 = \sqrt{1 + \beta^2} \cdot \sigma_{tot}$ . A  $\delta_{\perp}$  was then derived for the new pair of simulated datasets. This process was repeated for different values of  $\beta$ , resulting in predicted values of  $\delta_{\perp}$  as a function of  $\beta$ . For each dataset pair,  $\beta$  was then derived by comparing this function with the observed  $\delta_{\perp}$ . Note that by definition of  $\delta_{\perp}$  and  $\beta$ , this process is insensitive to details of the original sample such as number of points, sizes of individual errors, etc.

The results are listed in Table 3: All samples are characterized by non-statistical relative variabilities  $\beta > 10$ , with the Einstein-RASSBSC sample being the lowest as expected (due to the relatively large errors on the count rates); and despite the significantly higher  $\delta_{\perp}$  of the Einstein-WGACAT sample relative to the RASSBSC-WGACAT sample, the range of relative variabilities  $\beta$  overlap with each other, suggesting that long-term (potentially cyclic) variability is similar in magnitude to short-term (potentially episodic) variability.

The derived relative variabilities may also be used to estimate an “effective variability”,  $\frac{\Delta I}{I} \sim \beta / \langle SNR \rangle$ , where  $\langle SNR \rangle$  is an average measure of the signal-to-noise ratio. Inclusion of this factor further minimizes the stellar-distance bias in  $\beta$ . We thus derive (see Table 3)  $\frac{\Delta I}{I} = (0.29 - 0.36), (0.34 - 0.43), (0.41 - 0.52)$  for RASSBSC-WGACAT, Einstein-WGACAT, and Einstein-RASSBSC respectively. We note that the observed RASS and WGA count rates for FF Aqr are sharply different ( $\frac{RASS}{WGA} \sim 15$ ), and attribute this to a likely flare event during the *ROSAT* All-Sky Survey. This one star contributes  $\approx 10\%$  of the measured<sup>4</sup>  $\frac{\Delta I}{I}$ . The long-term

---

<sup>4</sup>We are potentially interested in detecting long-term cyclic variability, and hence would be justified in isolating

samples have systematically larger values of  $\frac{\Delta I}{I}$ , but are not significantly different given the size of the error bars, the possible systematic errors (see above), and the unsuitability of the adopted parameterization to characterize cyclic variability (see §3.3). Note that the measured “effective variability” over “short” timescales (RASSBSC-WGACAT) is similar to that found by Ambruster, Sciortino, & Golub (1987) by photon-arrival-time analysis of *Einstein* observations of selected stars over timescales ranging from  $\sim 10^2 - 10^3$  s. A similar result was also found by Pallavicini, Tagliaferri, & Stella (1990) in their analysis of *EXOSAT* data of flare stars: they detect variability at a variety of timescales ( $\sim 3^m - > 100^m$ ) in half the stars in their sample at strengths ranging from 15%-50%. Thus it might not be unreasonable to attribute most, and perhaps all, of the causes of the observed RASSBSC-WGACAT variability to processes (e.g., flares, rotational modulation, active region evolution) that operate on such relatively short timescales.

### 3.3. Cyclic Variability

Our modeling described above searches for stochastic (e.g., flaring) variability, and is insensitive to potential systematic (e.g., cyclic) variability in a sample where measurements of X-ray flux from individual stars are uncorrelated. However, if we compare the derived magnitude of the variability  $\frac{\Delta I}{I}$  in the short-term ( $\sim 1$  yr) with the long-term ( $\sim 10$  yr) samples, we do find indications of a larger variation over longer timescales. This result is statistically inconclusive since the error-bars on the variability indices ( $\frac{\Delta I}{I}$ ) derived for the various samples overlap, and further because of limitations imposed by the parameterization itself.

What fraction of the above variability is due to stochastic causes, and what fraction is due to the effects of periodic causes? In order to address this question, and thereby derive upper limits on the magnitude of a cyclic component to the variability, we model the flux variations as due entirely to a sinusoidal component combined with a constant base emission. We write the X-ray flux at an arbitrary time  $t$ ,

$$f_x(t) = A_{cyc} \sin\left(\frac{2\pi t}{P_{cyc}} + \phi\right) + A_{cyc} + f_{x_0}, \quad (2)$$

where  $A_{cyc}$  is the amplitude,  $P_{cyc}$  is the period, and  $\phi$  is the phase of the cyclic component, and  $f_{x_0}$  is a non-varying base emission. Note that  $f_x(t) \geq 0$  for all  $t$ . The strength of the cyclic activity may be parameterized by the ratio of cyclic to base emission fluxes,

$$\zeta = \frac{2A_{cyc}}{f_{x_0}}. \quad (3)$$

---

the effects of such variability by eliminating other contributors to the measured variability. Note however that we do not exclude FF Aqr from our analyses because we are unable to unambiguously identify cyclic variability in the chosen samples.

Conversely, if  $f_{obs}$  is the observed flux at, say,  $t = 0$ , and  $\zeta'$  is an estimated fraction of the cyclic component,

$$A_{cyc} = \frac{\zeta' f_{obs}}{2 + \zeta'(1 + \sin \phi)}. \quad (4)$$

We then estimate the maximum value that  $\zeta$  can have for our adopted sample of stars, using a technique similar to that used to measure the strength of stochastic variability (§3.1). In order to minimize the effects of short-term variability on estimates of cyclic variability, we model the cyclic variability *starting from* a paired dataset (say  $A$  and  $B$ ). The modeling involves obtaining monte carlo transpositions of the count rates of one the samples (say  $A$ ) to the epoch of a different sample (say  $C$ ). This transposition is carried out for a fixed value for the strength of the cyclic component (i.e.,  $\zeta = const.$ ), and using values of  $P_{cyc}$  randomly sampled from a log-normal distribution with a mean corresponding to 10 yr and  $1\sigma$  range corresponding to 4-25 yr (this range is a rough approximation of the results tabulated by Baliunas et al. 1995, based on the Mt. Wilson Ca II H+K monitoring program; see their Figure 3), at randomly selected phases, and including the effects of the error bars as in §3.1. A distribution of  $D_{\perp}/\sigma_{tot}$  is obtained as before for the paired datasets of the model ( $[A \rightarrow C](\zeta)$ ) and the original dataset ( $B$ ) – in other words, for the *simulated* pair  $B - C$  – and is compared with the distribution derived from the reference dataset of paired samples (here, the *observed* pair  $B - C$ ). The value of  $\zeta$  that minimizes the difference between the modeled and reference distributions of  $D_{\perp}/\sigma_{tot}$  indicates the level of cyclic variability required in order to account for the difference between the two pairs of datasets, *if* the entire difference is to be attributed to cyclic variability. The difference between the distributions is simply parameterized by the Kolmogorov-Smirnoff test statistic of the maximal distance  $\delta_{KS}(\zeta)$  between the cumulative distributions of  $D_{\perp}/\sigma_{tot}$ . Note that we do not attempt to derive a probability value for this statistic, partly because doing so implicitly assumes that the model adopted for transposing the count rates (Equation 2) is correct, and partly because the modeling is carried out via monte carlo simulations. Thus, we set an upper limit on the amplitude of the cyclic variability observable in the paired datasets  $B$  and  $C$ . Since we have three datasets, there are many combinations possible since each of RASSBSC, Einstein and WGACAT can correspond to all or any of  $A$ ,  $B$  and  $C$ . The curves illustrating the Kolmogorov-Smirnoff test statistic as a function of  $\zeta$  for two cases are illustrated in Figure 5.

The derived limit does depend on the sampling distribution adopted for the cyclic periods (see above): if longer periods are preferentially sampled (e.g., by increasing the width of the distribution, or by shifting it to longer periods), the upper limit on  $\zeta$  decreases – i.e., smaller cyclic amplitudes are sufficient to account for the entire change in the count rates of the samples studied – and vice versa. This trend is however weak when compared to the adopted distribution of  $P_{cyc}$ .

In order to investigate the cyclic component with greatest sensitivity, the observations obtained with longer time intervals between them need to be compared. In this case, our datasets  $A$ ,  $B$  and  $C$  corresponded to RASSBSC, WGACAT and Einstein, respectively. The function  $\delta_{KS}(\zeta)$  is illustrated for this case in Figure 5: considering paired samples of  $[RASSBSC \rightarrow Einstein](\zeta)$

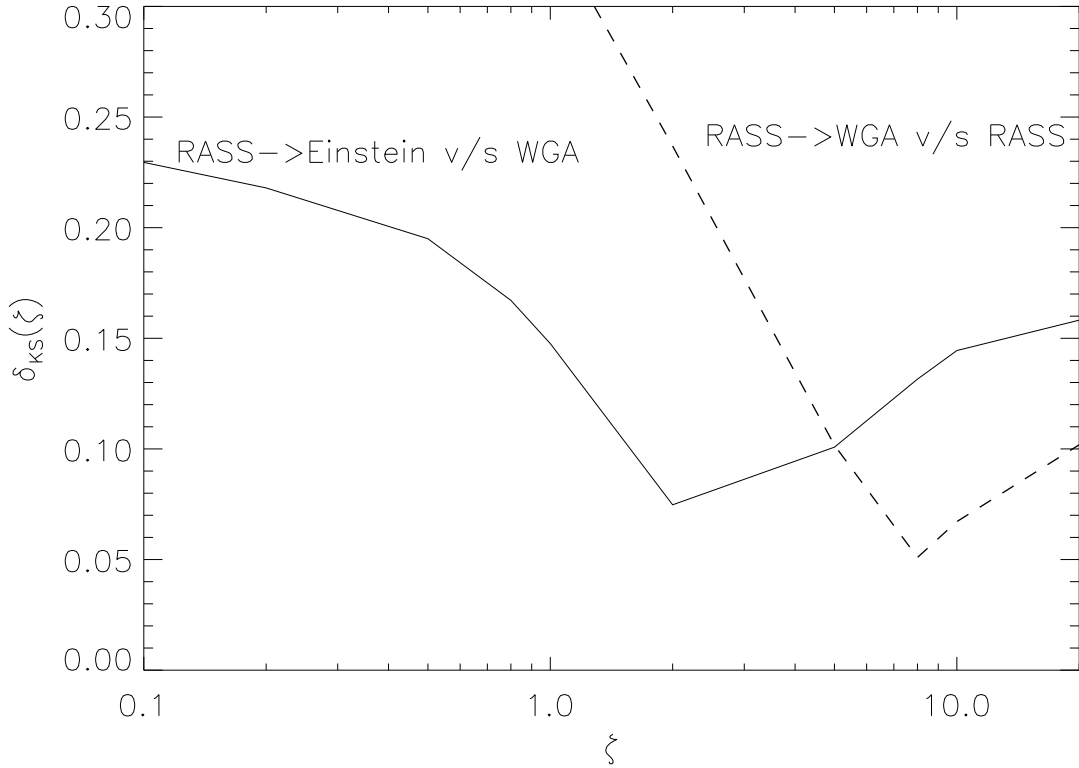


Fig. 5.— Magnitude of cyclic variability: The value of intrinsic cyclic amplitude that the selected set of stars must have in order that this variability is detectable. The maximal distance  $\delta_{KS}(\zeta)$  between the cumulative distributions of  $\delta_{\perp}$  for the modeled dataset and the reference dataset is shown for various values of the amplitude of cyclic variability for comparisons between observations separated by “long” (solid) and “short” (dashed) time intervals. The location of the minimum indicates the best model value that fits the data. The magnitude of cyclic variability present in the long-term (solid line) sample is  $\lesssim 2$ . Note that the error in  $\delta_{KS}(\zeta) \sim 0.03$ , and hence a better estimate for the amplitude of cyclic variability is  $\zeta \lesssim 4$ . In the case of the short-term sample (dashed line),  $\zeta \sim 10$ , which predicts variations that are much larger than observed over the long-term (cf. Figures 1-3). This latter result indicates that cycles alone *cannot* be responsible for the observed variability (see text).

and WGACAT (in other words, simulated Einstein-WGACAT) with a directly observed sample of Einstein-WGACAT, we find that the actual cyclic component must have a strength  $\zeta \lesssim 4$  – i.e., not more than 80% of the X-ray emission may be in the cyclic component even if all of the long-term variability is ascribed to the effects of activity cycles. It is worth noting here that we implicitly include the effects of short-term variability by using the RASSBSC-WGACAT sample as the initial distribution for modeling. The cyclic component is thus imposed on top of any variations that may exist due to flaring, and the effects of the latter are thus minimized.<sup>5</sup>

Also worthy of investigation is the magnitude of cyclic variability that might be required to explain *all* the additional (non-statistical) scatter between the RASSBSC and WGACAT samples – ie the assumption that there is no short-term or stochastic variability. For example, starting with a sample of RASSBSC stars alone, transposing them to the approximate WGACAT epoch for various values of  $\zeta$ , and considering the resultant paired sample of [RASSBSC→WGACAT]( $\zeta$ ) and RASSBSC, we find that only at large values of the cyclic component ( $\zeta \sim 10$ ) does the distribution match that derived from RASSBSC-WGACAT (Figure 5). However, such a large amplitude for cyclic variability would result in a much larger spread in count rates than is observed in our comparisons of Einstein vs. ROSAT datasets (Figures 1 and 2). This is as one would expect in the presence of significant short-term stochastic variability: indeed, it is telling us that the observed variability *cannot* only be of a cyclic nature. This constraint is only possible using observations obtained at three different epochs, as we have here.

It is interesting to compare our upper limit for  $\zeta$  for this sample of active binary stars to the observed cyclic component of solar coronal activity. In the case of the Sun, data obtained by *Yohkoh* have illustrated the very large contrast in soft X-rays between the Sun at solar minimum, essentially devoid of active regions, and at solar maximum when several large active regions are generally present on the visible hemisphere at any one time (e.g., Hara 1996, Acton 1996). The observed change in soft X-ray flux from solar minimum to maximum amounts to at least an order of magnitude (Aschwanden 1994, Acton 1996) and likely much larger (Kreplin 1970), so that a solar value for our parameter describing the cyclic activity component is  $\zeta_{\odot} \gtrsim 10$ .

Fleming et al. (1995) have carried out an analysis of X-ray variability using an X-ray selected sample, viz., RASS flux measurements of EMSS stars. They find that relative to F stars, 24% of Solar-type stars, 49% of dMe stars, and 19% of RS CVn and WUMa stars show a significant *decrease* in emission, while 12%, 10%, and 48% respectively of the above types show significant *increases*. The larger apparent decreases for normal stars may be ascribed to the bias inherent in X-ray selected stellar samples. In contrast, the apparent increase in the number of active binary stars showing increased emission levels cannot be due to such a bias. We are however unable to

---

<sup>5</sup>The structure of our chosen datasets do not allow us to distinguish between “flaring” and “quiescent” (which may arise due to active region evolution, rotational modulation, etc.) variability, a distinction made by Kürster et al. (1997) using periodogram analysis of the light curve of AB Dor; the “short-term” variability we refer to includes both types.



confirm this effect using a different, and larger, sample of stars that include EOSCAT and Slew observations. Indeed, for unbiased, uncorrelated, samples it is difficult to envision a physical mechanism that would cause this apparent increase found by them, and we therefore attribute it to accidental sample selection effects (as Fleming et al. also do) and to possible variations in flux calibration (see Figure 3 of Fleming et al).

Comparison of X-ray fluxes between *Einstein* and *ROSAT* epochs using statistically complete samples of field stars (Schmitt et al. 1995) shows that there is little evidence for systematic changes in the mean X-ray emission levels of stars in excess of factors of 2 on timescales of 10 yr. Schmitt et al. point out that this result is valid especially for active flare stars, but caution that the apparently larger spread in X-ray emission observed for fainter stars could be an artifact of the small number of such stars present in the sample.

Attempts to constrain long-term variability in X-ray emission from stars in the Pleiades (Schmitt et al. 1993, Gagné et al. 1995, Micela et al. 1996) and the Hyades (Stern et al. 1995) clusters have also been inconclusive. Schmitt et al. (1993) compare Pleiades stars detected in the *ROSAT* All-Sky Survey with previous *Einstein* observations and find numerous instances of strong variability by factors of an order of magnitude that are unlikely to be due to rotational modulation, measurement or calibration errors, or flaring activity; they conclude that cyclic activity must be the cause of such large variations. In contrast, Gagné et al. (1995) and Micela et al. (1996) find at best a marginal increase in long-term variability compared to short-term variability in their analyses of pointed data: the latter find that 15% of the stars show variability by factors  $> 2$  over  $\sim 10$  years and 10% over  $\frac{1}{2}$  year; the former find 40% of the stars show significant variability over 10 – 11 years compared to 25% over  $\frac{1}{2} - \frac{3}{2}$  years, but that the difference could be attributed to a bias resulting from the increased sensitivity of *ROSAT*. Stern et al. (1995) conclude from their comparison of *Einstein* and *ROSAT* data of the Hyades that the majority of the stars show long-term variability of less than a factor of 2, and that there is no evidence of strong cyclic activity. As noted above, this amplitude of variability is similar to what one would expect on short timescales of  $\lesssim 10^3$  s based on the time-series analyses of *Einstein* observations of various stars (Ambruster et al. 1987).

In this context, it must be noted that a long-term monitoring program of the young active K star AB Dor has been carried out with *ROSAT* by Kürster et al. (1997): they find that the X-ray flux is variable on short time-scales ranging from minutes to weeks, but shows no long-term trend indicative of cyclic activity over the  $5\frac{1}{2}$  years of the program. The lack of a detection of cyclic variability in this star of course does not rule out its presence in other active stars, and indeed may even manifest itself in AB Dor itself at much longer timescales.

Micela & Marino (1998) have compared the changes in X-ray emission in field dM stars observed with *ROSAT* over timescales of days to months, and have compared that data with similar data for the Sun by constructing maximum-likelihood distribution functions of the flux variations. They conclude that variability is present at all timescales they have considered, but do

not distinguish between long- and short-term or stochastic and cyclic variability. They have also applied their method to compare Pleiades dM star data from *Einstein*/IPC, *ROSAT*/PSPC, and *ROSAT*/HRI to Solar data and reach the same conclusion.

The problem of whether or not F-K main sequence stars in general are similar to the Sun in their trends of X-ray emission variations with magnetic cycles has been studied recently by Hempelmann et al. (1996). These authors attempted to circumvent the sparse X-ray observations of any one single star through a statistical study of a group of stars for which long-term Mt. Wilson Ca II H+K monitoring observations are available, and for which distinct cyclic activity behavior was detected (e.g., Baliunas et al. 1995 and references therein). They found that the *deviation* of X-ray surface fluxes  $F_x$  (derived from *ROSAT* all-sky survey and pointed phased observations) from the mean relation between  $F_x$  and Rossby number,  $R_o$ , is correlated with activity cycle phase as indicated by the Mt. Wilson Ca II H+K *S*-index.

In addition to stars with cyclic Ca II H+K emission, the Mt. Wilson monitoring program also revealed stars with less regular and more chaotic variability (Baliunas et al. 1995). Hempelmann et al. (1995) showed that the “regular” (cyclic) and “irregular” stars are strongly anti-correlated with the Rossby number,  $R_o$ ; the X-ray fluxes of the latter group clearly show them to comprise the most active stars with the highest surface fluxes. Hempelmann et al. interpreted these results in terms of a transition from a non-linear to a linear dynamo going from the irregular to the regular stars. This view is supported by non-linear modeling of stellar dynamos (e.g. Tobias, Weiss, & Kirk 1995, Knobloch & Landsberg 1996, and references therein) which show that as stellar rotation period is decreased, an initially steady system begins to exhibit quasi-periodicity or maunder-minimum type aperiodicity; chaotic behavior is a natural consequence of such models.

Alternately, Drake et al. (1996) argued that the observational evidence indicating both active stars and fully-convective M-dwarfs—the latter supposedly being unable to support a solar-like  $\alpha\omega$  dynamo—do not appear to show strong cyclic behavior provided empirical support for the qualitative theoretical framework outlined by Weiss (1993; see also Weiss 1996) in which the magnetic activity on active stars and low-mass fully-convective stars is predominantly maintained by a turbulent or distributed dynamo (e.g., Durney et al. 1993, Weiss 1993, Rosner et al. 1995). Stern et al. (1995; see also Stern 1998), in their comparison of *Einstein* and *ROSAT* observations of Hyades dG stars, made similar speculations. Small-scale magnetic fields generated by turbulent compressible convection within the entire convective zone (e.g., Nordlund et al. 1992, Durney et al. 1993) would result in different functional dependences of activity indicators with stellar parameters, and in particular, because of its disordered spatial and temporal nature, would not be expected to exhibit activity cycles (Cattaneo 1997).

In the above context, the general lack of well-defined activity cycles in the Ca II H and K emission of the most active stars is especially interesting in light of the very recent finding based on radio observations of a magnetic cycle on the rapidly rotating RS CVn binary UX Ari (G0 V + K0 IV; Period=6.44 day), with an apparent polarity reversal every 25.5 *days* (Massi et al. 1998).

If this surprisingly short period were analogous to the solar 22 year cycle, it would appear to offer a promising explanation for the lack of obvious cyclic behavior on timescales of years. However, the situation regarding cycles on RSCVn and other active stars is not quite so clear. Several authors have found evidence for cyclic behavior with periods comparable to that of the solar cycle on very active stars. For example, cycles of 11.1 yr for  $\lambda$  And, 8.5 yr for  $\sigma$  Gem, 11 yr for II Peg, and 16 yr for V711 Tau were inferred by Henry et al. (1995) from mean brightness changes derived from up to 19 years of photoelectric photometry. Dorren & Guinan (1994) find evidence for an activity cycle with a period of about 12 years on the rapidly rotating solar-like G dwarf EK Dra (HD 129333; rotation period  $\sim 2.8$  days). Rodonò et al. (1995) also find a periodic variation in the spot coverage of RSCVn with a period of about 20 years, while Lanza et al. (1998) find similar evidence for a 17 year activity cycle in the secondary of AR Lac. Alternatively, others have detected photometric variability, but failed to find firm evidence for cyclic behavior in numerous binaries (eg. Strassmeier et al. 1994 in the RSCVn star HR 7275; Oláh et al. 1997 in the case of HK Lac; Cutispoto 1993 in the case of IL Hya, LQ Hya, V829 Cen, V851 Cen, V841 Cen, GX Lib, V343 Nor, and V824 Ara).

Regardless of the observed periods of activity cycles of active binaries based on optical observations of modulation in, presumably, magnetically-related spot coverage, it is clear based on the results of our and earlier analyses that magnetic activity manifest in coronal X-ray emission is at best only weakly modulated by any long-term magnetic cycles present. This contrasts with the solar case in which coronal activity is very strongly dependent on the solar magnetic cycle. While we cannot rule out the existence of a multi-period cyclic dynamo, we suggest based on the relatively small difference between the short-term and long-term variabilities that this situation reinforces the earlier conclusions and conjectures of Stern et al. (1995), Drake et al. (1996) and Stern (1998) that a turbulent or distributed dynamo dominates the magnetic activity of the more active stars.

#### 4. Summary

In order to determine the characteristics of the variability of X-ray emission on active binary systems, we have carried out a statistical comparison of the X-ray count rates observed at different epochs. From the list of active chromosphere stars cataloged by Strassmeier et al. (1993) we have extracted subsamples which were detected in the following surveys: *Einstein*/IPC EOSCAT, EMSS, and Slew; *ROSAT* All-Sky Survey (RASSBSC); *ROSAT* archival pointed dataset (WGACAT). Our study differs from and improves upon earlier comparisons of *Einstein* and *ROSAT* observations of late-type stars in that the analysis of both RASSBSC and WGACAT observations enables us, at least in principle, to distinguish between “short” and long-term components of variability.

Assuming that the emission from separate stars are uncorrelated, we compute a measure of the relative departure from equality ( $\delta_{\perp}$ , Equation 1) for each combination of the above samples.

We show that the values of  $\delta_{\perp}$  thus derived are inconsistent with each other, i.e., there is evidence for non-statistical variations in the observed count rates of the sample stars in the different epochs.

We model the detected variability as stochastic variability, and conclude that the “effective variability” (an average value of the fractional variation in the observed count rate) is apparently the lowest for the samples separated by the shortest timescales (RASSBSC-WGACAT:  $\frac{\Delta I}{I} = 0.32^{0.36}_{0.29}$ ), and appears to be systematically larger for the samples separated by longer timescales (Einstein-RASSBSC:  $\frac{\Delta I}{I} = 0.46^{0.52}_{0.41}$ ; Einstein-WGACAT:  $\frac{\Delta I}{I} = 0.38^{0.43}_{0.34}$ ). This suggests the existence of a long-term component to the variability, but the evidence for such a component is marginal. If such a component exists, it could be due to stellar activity cycles strongly modified by X-ray emission arising due to relatively unmodulated small-scale fields generated by turbulent dynamos in the convective zone.

We model the long-term component as a sinusoidal cyclic variation atop a constant base emission, and constrain its strength by comparing simulated distributions of perpendicular deviations with observed distributions. We find that such a cyclic component, if it exists, may at most be 4 times as strong as a constant, base emission. This contrasts with the Solar case, where cyclic activity causes an increase in the soft X-ray emission by factors  $\gtrsim 10$  at activity maximum relative to the flux at activity minimum. We note earlier conclusions that the nature of coronal activity on active stars fits the scenario whereby the generation of magnetic fields whose dissipation is observed in the form of coronal heating and subsequent radiative loss is dominated by a turbulent or distributed dynamo, rather than by a solar-like  $\alpha\omega$  large-scale field dynamo. This scenario is essentially the same as that suggested by, e.g., Weiss (1993, 1996), based on qualitative theoretical arguments. Comparisons of past and future observations of stellar coronal emission at different epochs, such as those analyzed here, for larger samples of stars with different activity levels and different spectral types, will be invaluable in distinguishing between different dynamo models.

We would like to thank Alanna Connors, Steve Saar, Brian Wood, Frank Primini, and the referee for useful comments. This research has made use of the SIMBAD database, operated at CDS, Strasbourg, France. VK was supported by NASA grants NAG5-3173, NAG5-3189, NAG5-3195, NAG5-3196, NAG5-3831, NAG5-6755 and NAG5-7226 during the course of this research. JJD was supported by the AXAF Science Center NASA contract NAS8-39073.

Table 1: Active Binaries observed in X-rays

Number <sup>1</sup>	Name	<i>Einstein</i>			<i>ROSAT</i>		Spectral Type <sup>1</sup>	Distance <sup>3</sup> [pc]
		Slew <sup>2</sup>	EMSS <sup>2</sup>	EOSCAT <sup>2</sup>	RASSBSC <sup>2</sup>	WGACAT <sup>2</sup>		
3	5 Cet	...	...	5.6	...	...	wF/K1III	307.7
4	BD Cet	...	...	...	65.5	...	K1III	416.7
5	13 Cet A	...	...	...	1116.0	...	F7V/G4V	21.0
6	FF And	...	...	...	1022.0	...	dM1e/dM1e	23.8
7	ζ And	650.0	...	467.0	1797.0	...	/K1III	55.6
8	CF Tuc	300.0	...	394.0	...	...	G0V/K4IV	86.2
9	BD+25 161	...	...	...	240.9	...	G2V	215.5
10	AY Cet	1850.0	...	1516.0	3939.0	...	WD/G5III	78.5
11	UV Psc	250.0	...	219.0	924.5	...	G4-6V/K0-2V	63.0
12	CP-57 296	...	...	...	491.6	...	G6-8IV-IIIe	117.8
13	BI Cet	340.0	...	...	1520.0	...	G5V:/G5V:	65.7
14	AR Psc	...	...	686.0	4673.0	...	K2V/?	45.2
15	UV For	...	...	...	140.9	...	K0IV	130.4
16	BD+34 363	...	...	...	995.5	...	K0III	196.9
17	6 Tri	460.0	...	416.0	1023.0	...	F5/K0III	93.6
20	UX For	2220.0	...	...	1841.0	...	G5-8V/(G)	40.4
22	VY Ari	960.0	...	772.0	6792.0	3790.0	K3-4V-IV	44.0
23	BD+25 497	...	...	...	52.3	...	G4V/G6V	77.5
24	EL Eri	...	...	...	443.0	...	G8IV-III	219.3
25	LX Per	...	...	129.0	571.4	...	G0IV/K0IV	100.0
28	UX Ari	3500.0	...	4360.0	5859.0	7710.0	G5V/K0IV	50.2
29	V711 Tau	4020.0	...	4142.0	18970.0	8950.0	G5IV/K1IV	29.0
30	V837 Tau	...	...	...	3996.0	...	G2V/K5V	37.3
31	HR 1176	...	...	...	83.9	...	F2:V/G8III	106.3
33	CF Tau	...	...	21.5	...	...	F8	200 <sup>1</sup>
34	AG Dor	...	...	...	839.4	...	K1Vp	34.9
35	EI Eri	1980.0	...	1394.0	4409.0	...	G5IV	56.2
37	V818 Tau	...	...	520.0	236.9	218.0	G6V/K6V	46.7
38	BD+17 703	...	...	...	109.3	57.9	G4V/G8V	45.8
39	BD+14 690	90.0	...	94.1	197.1	123.0	G0V	46.6
40	vB 69	...	...	...	...	43.1	K0V	49.8
41	V492 Per	...	...	...	230.6	...	K1III	118.1
42	V833 Tau	730.0	...	524.0	2689.0	1380.0	dK5e	17.9
43	3 Cam	...	...	53.1	94.7	...	K0III	152.0
44	RZ Eri	120.0	...	109.4	238.2	265.0	Am/K0IV	185.2
45	V808 Tau	...	...	...	191.5	159.0	K3V/K3V	52.7
47	V1198 Ori	...	...	...	1364.0	...	G5IV	33.5
48	12 Cam	350.0	...	207.0	466.8	673.0	K0III	191.6
49	HP Aur	...	...	...	52.5	...	G8	...
50	CP-77 196	...	...	...	376.3	...	K1IIIp	179.5
51	α Aur	...	...	4222.0	23540.0	13300.0	G1III/K0III	12.9
52	BD+75 217	...	...	...	205.1	...	K0III	136.8
54	TW Lep	...	...	...	1609.0	...	F6IV/K2III	170.4
55	V1149 Ori	200.0	...	148.5	626.1	...	K1III	144.3
56	CD-28 2525	...	...	...	166.7	...	G1V	87.6
57	HR 2072	...	...	...	654.8	...	F/G5-8III	127.2
58	SZ Pic	...	...	...	454.2	...	G8V	194.9
59	HR 2054	...	...	...	607.0	417.0	G8III	178.9
60	CQ Aur	...	...	50.8	...	...	F5/K1IV	242.1
61	TY Pic	...	...	...	219.0	...	F/G8-K0III	286.5

Table 1: (Contd.) Active Binaries observed in X-rays

Number <sup>1</sup>	Name	<i>Einstein</i>			<i>ROSAT</i>		Spectral Type <sup>1</sup>	Distance <sup>3</sup> [pc]
		Slew <sup>2</sup>	EMSS <sup>2</sup>	EOSCAT <sup>2</sup>	RASSBSC <sup>2</sup>	WGACAT <sup>2</sup>		
62	OU Gem	230.0	...	287.0	1741.0	...	K3V/K5V	14.7
63	TZ Pic	...	...	...	165.5	...	K1IV-IIIp	175.7
64	W92/NGC2264	...	...	22.7	137.7	55.9	K0:IVp	900 <sup>1</sup>
65	SV Cam	...	...	...	408.0	509.0	G2-3V/K4V	85.0
66	VV Mon	...	...	34.4	147.2	...	G2IV/K0IV	178.9
67	Gl 268	...	...	40.8	257.0	...	dM5e/dM5e	6.4
68	SS Cam	...	...	37.0	58.5	...	F5V-IV/K0IV-III	323.6
69	HR 2814	...	...	...	353.7	...	F9.5VK3:V/(K5V	34.8
70	AR Mon	...	...	42.1	97.1	...	G8III/K2-3III	276.2
71	YY Gem	900.0	...	464.0	3697.0	2570.0	dM1e/dM1e	15.8
72	V344 Pup	...	...	...	214.8	...	K1III	111.4
73	$\sigma$ Gem	2090.0	...	1557.0	8081.0	7260.0	K1III	37.5
75	54 Cam	250.0	...	227.7	1347.0	...	F9IV/G5IV	101.6
76	LU Hya	...	...	...	184.1	...	K1IV	49.5
78	HR 3385	...	...	...	714.6	...	K0III	130.7
79	RU Cnc	...	...	23.1	107.3	...	F5IV/K1IV	331.1
80	RZ Cnc	140.0	...	149.2	66.1	...	K1III/K3-4III	307.7
81	TY Pyx	...	...	...	1604.0	1930.0	G5IV/G5IV	55.8
83	XY UMa	...	...	...	...	2.9	G3V/(K4-5V)	150.8
84	BF Lyn	860.0	...	...	2908.0	...	K2V/(dK)	24.3
85	IL Hya	...	...	...	1703.0	...	K1III	119.6
86	IN Vel	...	...	...	120.8	...	K2IIIp	285.7
87	DH Leo	970.0	...	...	2053.0	...	K0V/K7VK5V	32.4
88	XY Leo B	...	...	96.9	368.1	258.0	M1V/M3V	63.1
89	BD+61 1183	...	...	...	347.8	...	G8IV	174.5
90	LR Hya	...	...	...	79.9	64.0	K0V/K0V	33.8
91	DM UMa	570.0	...	...	897.1	...	K0-1IV-III	138.7
92	$\xi$ UMa B	2580.0	...	873.0	4539.0	...	G5V	8 <sup>1</sup>
95	CD-38 7259	...	...	...	928.6	...	G5V/K1IV	121.7
96	HR 4492	1290.0	...	...	2959.0	...	A0/K2-4III	172.1
97	RW UMa	170.0	...	89.3	78.2	...	F8IV/K0IV	242.1
98	93 Leo	410.0	...	259.0	1122.0	...	A6:V/G5IV-III	69.4
99	HU Vir	...	...	...	428.9	...	K0IV	125.0
100	HR 4665	580.0	...	606.0	1638.0	...	K1III/K1III	138.1
101	AS Dra	...	...	80.0	236.4	...	G4V/G9V	43.2
102	IL Com	...	68.1	71.0	600.1	488.0	F8V/F8V	107.1
103	BD+25 2511	...	...	...	201.2	241.0	$\iota$ G9V $\iota$	55 <sup>1</sup>
104	BD-05 3578	...	63.6	28.0	228.8	203.0	G5V/(K-M)	1204.8
105	IN Com	...	...	...	...	6.2	G5IV-III	190.8
106	BD+47 2007	...	...	...	395.0	381.0	F/K0III	190.8
107	UX Com	120.0	...	50.2	196.5	...	G2/K1(IV)	168.4
108	BD-4 3419	...	...	...	193.6	...	K2IV-III	300.3
109	RS CVn	380.0	...	390.0	886.2	634.0	F4IV/G9IV	108.1
110	HR 4980	...	...	...	756.7	...	G0V/G0V	39.8
111	BL CVn	...	...	...	71.5	...	G-KIV/K0III	284.9
112	BM CVn	...	...	...	1316.0	...	K1III	111.1
114	HR 5110	1200.0	...	1542.0	2768.0	4580.0	F2IV/K2IV	44.5
115	CD-32 9477	...	...	46.3	127.0	144.0	K2IIIp	507.6
116	V851 Cen	680.0	...	551.0	1303.0	...	K2IV-III	76.2
117	BH Vir	...	...	...	164.9	...	F8V-IV/G2V	125.9

Table 1: (Contd.) Active Binaries observed in X-rays

Number <sup>1</sup>	Name	<i>Einstein</i>			<i>ROSAT</i>		Spectral Type <sup>1</sup>	Distance <sup>3</sup> [pc]
		Slew <sup>2</sup>	EMSS <sup>2</sup>	EO SCAT <sup>2</sup>	RASSBSC <sup>2</sup>	WGACAT <sup>2</sup>		
118	V841 Cen	...	...	...	800.8	669.0	K1IV	63 <sup>1</sup>
119	RV Lib	...	...	60.4	160.5	...	G8IV/K3IV	370.4
120	HR 5553	...	...	78.0	362.9	294.0	K2V	11.5
121	SS Boo	...	...	47.3	64.0	75.3	G0V/K0IV	202.0
122	UV CrB	...	18.1	17.9	...	...	K2III	279.3
123	GX Lib	...	34.1	33.3	138.1	...	(G-KV)/K1III	95.1
124	LS TrA	...	...	...	1189.0	...	K2IV/K2IV	127.4
126	RT CrB	...	...	10.7	...	...	G2/G5-8IV	1428.6
128	1E1548.7+1125	...	28.8	28.4	...	127.0	K5V-IV	500 <sup>1</sup>
130	MS Ser	300.0	...	85.1	642.6	...	K2V/K6V	87.8
131	BD+11 2910	...	...	...	359.2	...	G8IV	40.3
132	$\sigma^2$ CrB	2270.0	...	2170.0	9487.0	8710.0	F6V/G0V	21.7
134	CM Dra	...	...	...	176.7	...	M4Ve/M4Ve	15 <sup>1</sup>
136	WW Dra	350.0	...	84.2	493.3	...	G2IV/K0IV	115.3
137	$\epsilon$ UMi	...	...	...	1048.0	...	A8-F0V/G5III	106.3
138	CD-26 11634	...	...	...	372.3	...	K0III	471.7
139	V792 Her	...	...	184.0	365.6	...	F2IV/K0III	413.2
141	V824 Ara	...	...	...	4758.0	...	G5IV/K0V-IV	31.4
142	HR 6469	...	...	...	174.9	...	F2V/ G0V G5IV	64.4
143	V965 Sco	...	...	...	200.3	144.0	F2IV/K1III	406.5
144	29 Dra	800.0	...	...	1272.0	2320.0	WD/K0-2III	103.3
146	BD+36 2975	...	...	...	1875.0	...	G6V/K1IV	30.9
147	Z Her	...	...	113.0	...	...	F4V-IV/K0IV	98.3
148	MM Her	...	...	64.3	133.7	...	G2/K0IV	184.5
149	V772 Her	...	...	542.9	2886.0	1890.0	G0V/ M1V G5V	37.7
150	ADS 11060C	...	...	542.9	2886.0	1890.0	K7:V/K7V	37.7
151	V832 Ara	...	...	...	233.9	237.0	WD/G8III	266.7
152	V815 Her	...	...	...	3113.0	...	G5V/(M1-2V)	32.6
153	PW Her	...	...	43.2	116.7	...	F8-G2/K0IV	232.0
155	AW Her	...	...	35.6	88.4	...	G2/G8IV	212.3
156	BY Dra	1020.0	...	556.0	2414.0	1460.0	K4V/K7.5V	16.4
157	1E1848+3305	...	...	51.6	166.7	...	K0III-IV	229 <sup>1</sup>
158	1E1848+3325	...	...	16.7	...	...	G5V	95 <sup>1</sup>
159	$\sigma$ Dra	...	...	16.6	50.5	...	G9III	98.8
160	V1285 Aql	...	...	159.5	1392.0	...	M3.5Ve/M3.5Ve	11.6
161	V775 Her	...	...	...	1878.0	1640.0	K0V/(K5-M2V)	21.4
162	V478 Lyr	...	...	...	2095.0	...	G8V/(dK-dM)	28.0
163	HR 7275	810.0	...	788.0	1275.0	...	K1IV-III	70.2
164	1E1919+0427	...	...	29.1	126.5	...	G5V/K0III-IV	95 <sup>1</sup>
165	V4138 Sgr	...	...	...	1345.0	...	K1III	87.7
166	V4139 Sgr	...	...	...	100.3	...	K2-3III	240.4
167	HR 7428	...	...	76.0	107.9	131.0	A2V/K2III-II	322.6
169	1E1937+3027	...	...	21.5	...	88.8	K0III-IV	229 <sup>1</sup>
171	HR 7578	...	...	...	415.9	...	K2-3V/K2-3V	14.2
173	BD+15 4057	...	...	...	179.7	...	G5V/G5V	55.8
174	BD+31 4046	...	...	...	239.0	...	K0III	275 <sup>1</sup>
175	BI Del	...	...	...	82.7	...	K0	...
176	AT Cap	...	...	...	67.1	...	K2III	99 <sup>1</sup>
177	CG Cyg	...	...	...	143.1	...	G9.5V/K3V	108.1
178	V1396 Cyg	410.0	...	...	1013.0	...	M2V/M4Ve	15.1

Table 1: (Contd.) Active Binaries observed in X-rays

Number <sup>1</sup>	Name	<i>Einstein</i>			<i>ROSAT</i>		Spectral Type <sup>1</sup>	Distance <sup>3</sup> [pc]
		Slew <sup>2</sup>	EMSS <sup>2</sup>	EOSCAT <sup>2</sup>	RASSBSC <sup>2</sup>	WGACAT <sup>2</sup>		
179	ER Vul	570.0	...	391.0	2310.0	1670.0	G0V/G5V	49.9
181	BD+10 4514	...	...	...	262.7	...	F9V/G0VGIV	50.5
182	HR 8170	...	...	...	729.2	638.0	F8V/wK5V	26.6
183	BH Ind	...	...	...	345.6	...	K1IIICNIVp	310.6
184	BD-00 4234	...	...	...	388.6	...	K3Ve/K7Ve	49.4
185	AS Cap	...	...	...	326.5	...	K1III	204.1
186	AD Cap	...	...	137.0	305.6	...	G5-8IV-V/G5	191.6
187	42 Cap	...	...	...	639.0	...	G2IV	32.5
188	FF Aqr	...	...	...	5346.0	335.0	sdO-B/G8IV-III	126.4
189	RT Lac	120.0	...	110.5	141.9	224.0	G5-/G9IV	192.7
190	HK Lac	300.0	...	357.0	1463.0	...	F1V/K0III	151.1
191	AR Lac	1860.0	...	1268.0	7786.0	4010.0	G2IV/K0IV	42.0
192	WW Cep	...	...	...	158.3	...	K0	...
193	BD+29 4645	...	...	...	932.6	...	F5-8/G8IV	145.1
194	V350 Lac	...	...	163.0	670.0	...	K2III	122.2
195	FK Aqr	660.0	...	787.0	3803.0	...	dM2e/dM3e	8.6
196	IM Peg	...	...	585.0	2505.0	3730.0	K2III-II	96.8
198	TZ PsA	450.0	...	...	792.4	...	G5Vp	65.8
199	KU Peg	...	...	...	173.2	...	G8II	187.6
200	KZ And	540.0	...	366.0	1928.0	1540.0	dK2/dK2	25.3
201	RT And	...	...	...	224.2	...	F8V/K0V	75.4
202	SZ Psc	...	...	976.0	4463.0	...	F8IV/K1IV	88.2
203	EZ Peg	...	...	...	679.1	438.0	G5V-IV/K0IV:	129.5
204	$\lambda$ And	2850.0	...	2080.0	9822.0	6000.0	G8IV-III	25.8
205	KT Peg	...	...	...	363.7	...	G5V/K6V	49.3
206	II Peg	2980.0	...	1156.0	10900.0	9040.0	K2-3V-IV	42.3

NOTES:-

1. as in Strassmeier et al. (1993).
2. Vignetting-corrected count-rates [ct ks<sup>-1</sup>].
3. from Hipparcos catalog (Perryman et al. 1997)

Table 2: Corelation Tests

	Einstein-RASSBSC	Einstein-WGACAT	RASSBSC-WGACAT
Sample Size	83	35	47
Pearson Coefficient	0.84	0.89	0.94
Spearman's $\rho$	0.91	0.94	0.97
Kendall's $\tau$	0.73	0.79	0.86

Table 3: Measured Variability

	Einstein-RASSBSC	Einstein-WGACAT	RASSBSC-WGACAT
$\delta_{\perp}$	$4.38 \pm 0.07$	$6.62 \pm 0.11$	$5.33 \pm 0.09$
$\beta$	$12 \begin{smallmatrix} >11 \\ <14 \end{smallmatrix}$	$20 \begin{smallmatrix} >17 \\ <22 \end{smallmatrix}$	$15 \begin{smallmatrix} >13 \\ <17 \end{smallmatrix}$
$\frac{\Delta I}{I}$	$0.46 \begin{smallmatrix} >0.41 \\ <0.52 \end{smallmatrix}$	$0.38 \begin{smallmatrix} >0.34 \\ <0.44 \end{smallmatrix}$	$0.32 \begin{smallmatrix} >0.29 \\ <0.37 \end{smallmatrix}$



## REFERENCES

- Acton, L. 1996, in “Cool Stars, Stellar Systems, and the Sun, 9<sup>th</sup> Cambridge Workshop,” eds. R.Pallavicini & A.K.Dupree, ASP Conf. Ser., 109, 45
- Ambruster, C.W., Sciortino, s., & Golub, L. 1987, ApJS, 65, 273
- Aschwanden, M. 1994, Sol.Phys., 152, 53
- Ayres, T.R., Simon, T., Stauffer, J.R., Stern, R.A., Pye, J.P., & Brown, A. 1996, ApJ, 473, 279
- Baliunas, S.L. et al., 1995, ApJ, 438, 269
- Cattaneo, F. 1997, in “SCORE’96: Solar Convection and Oscillations and their Relationship,” eds. F.P.Pijpers, J.Christensen-Dalsgaard, & C.S.Rosenthal, Kluwer:Dordrecht, 201
- Cutispoto, C. 1993, A&AS, 102, 655
- Dempsey, R.C., Linsky, J.L., Schmitt, J.H.M.M., & Fleming, T.A. 1993, ApJ, 413, 333
- Dorren, J.D., & Guinan, E.F. 1994, ApJ, 428, 805
- Drake, J.J., Stern, R.A., Stringfellow, G.S., Mathioudakis, M., Laming, J.M., & Lambert, D.L. 1996, ApJ, 469, 828
- Durney, B.R., De Young, D.S., & Roxburgh, I.W. 1993, Sol.Phys., 145, 207
- Elvis, M., Plummer, D., Schachter, J., & Fabbiano, G. 1992, ApJS, 80, 257
- Fleming, T.A., Molendi, S., Maccacaro, T., & Wolter, A. 1995, ApJS, 99, 701
- Gagné, M., Caillault, J.-P., & Stauffer, J.R. 1995, ApJ, 450, 217
- Gioia, I.M., Maccacaro, T., Schild, R.E., & Wolter, A. 1990, ApJS, 72, 567
- Hara, H. 1996, in “Magnetodynamic Phenomena in the Solar Atmosphere—Prototypes of Stellar Magnetic Activity”, eds. Y.Uchida, T.Kosugi, & H.S.Hudson, Kluwer:Dordrecht, 321
- Harris, D.E. et al. 1990, FITS/CD-ROM v1, SAO publication
- Harvey, K. 1992, in “The Solar Cycle,” ASP Conf. Series, Ed. K.L.Harvey, v.27, p.335
- Hempelmann, A., Schmitt, J.H.M.M., & Stepièn, K., 1995, A&A, 305, 284
- Henry, G.W., Eaton, J.A., Hammer, J., & Hall, D.S., 1995, ApJS, 97, 513
- Knobloch, E., & Landsberg, A.S. 1996, MNRAS, 278, 294
- Kreplin, R.W. 1970, Ann. Géophys., 26, 567
- Kuerster, M., Schmitt, J.H.M.M., Cutispoto, G., & Dennerl, K. 1997, A&A, 320, 831
- Lanza, A.F., Catalano, S., Cutispoto, G., Pagano, I., & Rodonó, M. 1998, A&A, 332, 541
- Massi, M., Neidhofer, J., Torricelli-Ciampioni, G., & Chiuderi-Drago, F., 1998, A&A, 332, 149
- Micela, G., & Marino, A. 1998, in the Proceedings of the meeting *Very Low-Mass Stars and Brown dwarfs in Stellar Clusters and Associations*, La Palma, in press

- Micela, G., Sciortino, S., Kashyap, V., Harnden, F.R., Jr. & Rosner, R. 1996, *ApJS*, 102, 75
- Nordlund, Å., Brandenburg, A., Jennings, R.L., Rieutord, M., Ruokolainen, J., Stein, R.F., & Tuominen, I. 1992, *ApJ*, 392, 647
- Oláh, K., Kövári, Zs., Bartus, J., Strassmeier, K.G., Hall, D.S., & Henry, G.W., 1997, *A&A*, 321, 811
- Pallavicini, R. 1993, in “Physics of Solar and Stellar Coronae: G.S.Vaiana Memorial Symposium,” eds. J.F.Linsky and S.Serio, Kluwer: Utrecht, p.237
- Pallavicini, R., Tagliaferri, G., & Stella, L. 1990, *A&A*, 228, 403
- Perryman, M.A.C., et al. 1997, *A&A*, 323, 49
- Plummer, D., Schachter, J., Elvis, M., & McDowell, J. 1994, BINTABLE/CD-ROM v1.1, SAO/NASA publication
- Press, W.H., Teukolsky, S.A., Vetterling, W.T., & Flannery, B.P. 1992, “Numerical Recipes in C: The Art of Scientific Computing,” 2<sup>nd</sup> Edition, Cambridge University Press, 703
- Rodonó, M., Lanza, A.F., & Catalano, S. 1995, *A&A*, 301, 75
- Rosner, R., Musielak, Z.E., Cattaneo, F., Moore, R.L., & Suess, S.T. 1995, *ApJ*, 442, L25
- Saar, S.H., & Baliunas, S.L. 1992, in “The Solar Cycle,” ASP Conf. Series, Ed. K.L.Harvey, v.27, p.150
- Schmitt, J.H.M.M., Collura, A., Sciortino, S., Vaiana, G.S., Harnden, F.R., Jr., Rosner, R. 1990, *ApJ*, 365, 704
- Schmitt, J.H.M.M., Kahabka, P., Stauffer, J., & Pitters, A.J.M. 1993, *A&A*, 277, 114
- Schmitt, J.H.M.M., Fleming, T.A., & Giampapa, M.S. 1995, *ApJ*, 450, 392
- Stern, R.A. 1998, in “Cool Stars, Stellar Systems, and the Sun, 10<sup>th</sup> Cambridge Workshop,” eds. R.A.Donahue & J.Bookbinder, ASP Conf. Ser., 154, 223
- Stern, R.A., Schmitt, J.H.M.M., Kahabka, P.T. 1995, *ApJ*, 448, 683
- Stocke, J.T., Morris, S.L., Gioia, I.M., Maccacaro, T., Schild, R.E., Wolter, A., Fleming, T.A., & Henry, J.P. 1991, *ApJS*, 76, 813
- Strassmeier, K.G., Hall, D.S., Fekel, F.C., & Scheck, M. 1993, *A&AS*, 100, 173
- Strassmeier, K.G., Hall, D.S., & Henry, G.W. 1994, *A&A*, 282, 535
- Tobias, S.M., Weiss, N.O., & Kirk, V. 1995, *MNRAS*, 273, 1150
- Vaiana, G.S., & Rosner, R. 1978, *ARAA*, 16, 393
- Vaiana, G.S., et al., 1981, *ApJ*, 244, 163
- Voges W., Gruber R., Haberl F., Kuerster M., Pietsch W., & Zimmermann U., 1994, in *ROSAT News No.32*
- Voges, W. et al. 1996, *IAU Circ.* 6420

Vogt, S.S., & Penrod, G.D., 1983, *PASP*, 95, 565

Weiss, N.O. 1993, in “Physics of Solar and Stellar Coronae: G.S.Vaiana Memorial Symposium,” eds. J.F.Linsky and S.Serio Kluwer:Dordrecht, p.541

Weiss, N.O. 1996, in “Magnetodynamic Phenomena in the Solar Atmosphere—Prototypes of Stellar Magnetic Activity”, eds. Y.Uchida, T.Kosugi, & H.S.Hudson, Kluwer:Dordrecht, 387

White, N.E., Giommi, P., & Angelini, L. 1994, *IAU Circ.* 6100

Wood, B.E., Brown, A., & Linsky, J.L. 1995, *ApJ*, 438, 350